ELSEVIER

Contents lists available at ScienceDirect

Chemical Engineering Journal

journal homepage: www.elsevier.com/locate/cej



Enhanced adsorption performance for selected pharmaceutical compounds by sonicated $Ti_3C_2T_X$ MXene



Sewoon Kim^a, Farivash Gholamirad^b, Miao Yu^c, Chang Min Park^d, Am Jang^e, Min Jang^f, Nadar Taheri-Oazvini^{b,g}, Yeomin Yoon^{a,*}

- ^a Department of Civil and Environmental Engineering, University of South Carolina, Columbia, 300 Main Street, SC 29208, USA
- Department of Chemical Engineering, University of South Carolina, Columbia, SC 29208, USA
- ^c Department of Chemical and Biological Engineering, Rensselaer Polytechnic Institute, Troy, NY 12180, USA
- d Department of Environmental Engineering, Kyungpook National University, 80 Daehak-ro, Buk-gu, Daegu 41566, Republic of Korea
- e School of Civil and Architecture Engineering, Sungkyunkwan University, 2066 Seobu-ro, Jangan-16 Gu, Suwon, Gyeonggi-do 16419, Republic of Korea
- f Department of Environmental Engineering, Kwangwoon University, 447-1, Wolgye-Dong Nowon-Gu, Seoul 01897, Republic of Korea
- ^g Biomedical Engineering Program, University of South Carolina, Columbia, SC 29208, USA

HIGHLIGHTS

- This study explored the removal of selected pharmaceuticals by Ti₃C₂T_X MXene.
- The highest removal was observed for a cationic pharmaceutical.
- The removal was significantly enhanced by sonicated MXene.
- MXene had relatively high selectivity compared to powdered activated carbon.
- The reusability of sonicated MXene is better than that of pristine MXene.

ARTICLE INFO

$\it Keywords$: $\it Ti_3C_2T_X$ MXene Pharmaceuticals Sonication Adsorption Water treatment

ABSTRACT

This paper is aimed at evaluating the feasibility of selected pharmaceutical compounds' adsorption on Ti₃C₂T_X MXene (termed 'MXene' in this study) as the first attempt. For adsorption mechanism analysis, amitriptyline (AMT), verapamil, carbamazepine, 17 α-ethinyl estradiol, ibuprofen, and diclofenac were the selected pharmaceutical compounds and experiments were conducted in three different pH conditions (3.5, 7, and 10.5). Due to electrostatic attraction between negatively charged MXene and positively charged AMT, the adsorption capacity for AMT showed the highest value (58.7 mg/g) at pH 7. In addition, for enhanced adsorption performance, MXene sonicated at different frequencies (0, 28, and 580 kHz) was applied for AMT adsorption. The maximum adsorption capacity was observed in the following order: 28 kHz (214 mg/g) > 580 kHz (172 mg/ g) > 0 kHz (138 mg/g). This is because cavitation bubbles by sonication can make well-dispersed MXene and more forming oxygenated functional groups on MXene. In particular, by generating larger cavitation bubbles, the highest performance was shown at lower frequencies. Furthermore, because there are a lot of ions in real aquatic environments, the effect of various ions on adsorption performance on pharmaceutical compounds was evaluated using sonicated MXene. Although background inorganics negatively affect adsorption performance, natural organic matter as background organics increased the adsorption performance. However, cetylpyridinium chloride (CPC), a major cationic surfactant of the pharmaceutical industry, had a negative effect on adsorption performance by exhibiting a competition effect between CPC and pharmaceutical compounds. Finally, a comparison between sonicated MXene and commercial powdered activated carbon and recyclability performances indicated that sonicated MXene could be an alternative adsorbent for pharmaceutical compounds removal due to its high adsorption capacity, selectivity, and reusability.

E-mail address: yoony@cec.sc.edu (Y. Yoon).

^{*} Corresponding author.

1. Introduction

Contaminants of emerging concern (CECs), including pharmaceutical compounds, personal care products, and endocrine-disrupting compounds, have been found at trace levels in most aquatic environments [1]. Due to a variety of anthropogenic impacts such as overpopulation, rapid urbanization, and climate change, these contaminants have been hugely consumed and overused by humans and industry. Particularly, pharmaceutical compounds, which are widely used in the prevention and treatment of human and animal diseases, are increasing in demand in line with improvements in standards of living [2]. The pharmaceutical compounds present in water can cause adverse effects on plants, animals, and human health due to their persistence, toxicity, and mobility [3,4]. The United States Environmental Protection Agency recently reported 109 types of pharmaceutical compounds detected in surface water around Denver, Colorado in 2018 [5]. In addition, the United States Geological Survey reported that 103 types of pharmaceutical compounds were found in groundwater used for drinking in the United States in 2019 [6]. Moreover, several other studies indicated that conventional water and wastewater treatment plants cannot properly remove the pharmaceutical compounds, leading to the release of various pharmaceutical compounds, including effluents into various water resources [7-9]. In other words, pharmaceutical compounds found in water present a number of contemporary water issues.

Among various other methods proposed to be used to remove pharmaceutical compounds to facilitate safer water resources, adsorption has been considered a promising technology due to its ease of operation, flexibility, safe generation of byproducts, and low energy demand [10,11]. In addition, adsorbent can be readily removed either by sedimentation or sand filtration in conventional drinking water treatment. Powdered activated carbon (PAC) as an adsorbent has been used in most adsorption systems to effectively treat a wide range of CECs [12]. Nevertheless, a number of studies indicate that there are limitations to PAC adsorption such as relatively poor polar compounds adsorption, slow kinetics, and easy complexation with natural organic matter (NOM) [13–15]. For these reasons, competitive adsorbents have been developed and applied to achieve the removal of CECs, such as pharmaceuticals compounds, from water.

Two-dimensional (2D) materials are members of the rapidly-expanding material family and have been applied for water purification purposes as well as material science due to their unique physicochemical properties [16,17]. Among them, Ti₃C₂T_X MXenes, which is a very recently discovered family of multilayered 2D transition metal carbides, have been in the spotlight in the adsorption area [17,18]. Due to its superior oxidation resistance, a fine structure, hydrophilicity, and the excellent stability of MXene, numerous researchers have tried to remove contaminants using this material as an adsorbent. Although these studies successfully demonstrated its removal performance, MXene has been used to remove mostly inorganic contaminants and only limited organic contaminants, including urea and dyes [17,19-21]. Therefore, there are still demands for studies into various organic contaminants' adsorption, such as pharmaceutical compounds. Furthermore, as it is still an early stage of MXene application, there is a lack of attempts to enhance the MXene adsorption process. For example, it has been reported that well-dispersed and smaller particle size adsorbate by sonication can show better adsorption capacity by keeping their specific characteristics and higher surface area in even changed water conditions [22,23].

The main purpose of this study is to assess the ability of MXene as adsorbent in the adsorption of pharmaceutical compounds in drinking water treatment. For removal performance and mechanism analysis, adsorption experiments were conducted for selected pharmaceutical compounds by ${\rm Ti}_3{\rm C}_2{\rm T}_{\rm X}$ MXene (as pristine MXene, termed 'P-MXene' in this study) at three different pH conditions. In addition, sonicated MXene at 28 and 580 kHz (termed 'S₂₈-MXene' and 'S₅₈₀-MXene', respectively) was applied to enhance adsorption performance. Sonication

which can produce the mechanical waves by using ultrasonic probes/horns or ultrasonic bath, has been commonly used to inhibit aggregation of adsorbent [24]. Sonication effects were identified by adsorption kinetics, isotherm, and characteristics change of sonicated MXene. Furthermore, adsorption performance was confirmed to evaluate effect of various background inorganics and organics. Additionally, by comparing adsorption performance between sonicated MXene and commercial PAC, we support the superiority of sonicated MXene as an adsorbent for the removal of pharmaceutical compounds. Finally, the regeneration possibility of P-MXene and sonicated MXene was investigated for the practical aspects of MXene's adsorption application.

2. Materials and methods

2.1. Chemicals

To receive a universal result, commercially available $Ti_3C_2T_X$ MXene was obtained from the Advanced Materials Development Expert Store (Hangzhou, Zhejiang, China). It was washed with de-ionized (DI) water (\sim 18.2 M Ω -cm) until pH reached approximately 6 and applied as P-MXene. Pharmaceutical compounds amitriptyline (AMT), verapamil (VRP), carbamazepine (CBM), 17 α -ethinyl estradiol (EE2), ibuprofen (IBP), and diclofenac (DCF) were selected and purchased from Sigma-Aldrich (St. Louis, MO, USA). Different physicochemical characteristics of these compounds were described in Table S1. Background inorganics, including NaCl, NaHCO $_3$, NaNO $_3$, Na $_2$ SO $_4$, and CaCl $_2$, and background organics, including HA, TA, and CPC were obtained from Sigma-Aldrich (St. Louis, MO, USA) for their effects on various water qualities. Lastly, for adsorption capacity comparison, commercial PAC was purchased from Evoqua Water Technologies, Randolph, MA, USA.

2.2. Characterization

The shapes and structures of the P-MXene were confirmed by scanning electron microscopy (SEM; S-4200, Japan), transmission electron microscopy (TEM; Titan G2, USA), and X-ray diffractometry (XRD; D/max-2500, Japan). In addition, for hydrodynamic diameters (D_h) of sonicated MXene, dynamic lighting scatters (DLS; ALV/CG3, Germany) were used with a high-QE APD detector. Furthermore, Fourier-transform infrared spectroscopy (FTIR; Frontier, USA) for chemical bonds, X-ray photoelectron spectroscopy (XPS, Quantera SXM, Japan) for chemical compositions, a zeta-potential analyzer (Zetapals, USA) to measure surface charge, and TEM for morphology were analyzed to measure changes in the properties of sonicated MXene.

2.3. Adsorption procedure

All the adsorption experiments were conducted using a 40 mL amber vial in duplicate at room temperature. In addition, all samples were filtered with a 0.22 μ m syringe filter before analysis. The results were measured using high-performance liquid chromatography (HPLC; 1200 series, USA) with ultraviolet (UV) or fluorescence detector. The HPLC analysis parameters followed reported literature for AMT and VRP [25] with some modification and our previous study for CBM, EE2, IBP, and DCF [26].

To observe the adsorption mechanism, 40 mg/L P-MXene was added into 10 μM of selected pharmaceutical compounds, each at three different pH conditions for 3 days. The pH value of the suspension was controlled with 0.1–1 M HCl and 0.1–1 M NaOH. To improve adsorption performance, the MXene was used after sonication at 28 and 580 kHz for 30 min. Adsorption kinetics were carried out for 0–720 min contact time with 40 mg/L adsorbents and 10 μM pharmaceuticals. For adsorption isotherm, 40 mg/L adsorbents were used with 5, 10, 20, 35, 55, and 80 μM pharmaceuticals as initial concentration for 2 h. The effect of various water qualities on adsorption capacity was investigated in the presence of background inorganics and background organics.

Desorption procedure of the adsorbed pharmaceutical compounds from adsorbents followed reported studies [27] with some modification by adding 0.1 M HCl for 2 h, 0.1 M NaOH for 2 h, DI water rinsing, and oven drying in sequences. Finally, adsorption performance, including adsorption capacity, removal rate, kinetics including pseudo-first-order (PFO) and pseudo-second-order (PSO) models, and isotherm including Langmuir, Freundlich, and Redlich-Peterson (R-P) models were employed to analyze results and described in the supporting information in detail.

3. Results and discussion

3.1. Adsorption performance and mechanism

Before evaluating adsorption performance, the morphology and crystalline phase of the P-MXene were identified, as shown in Fig. S1. The TEM/SEM images and XRD patterns indicate well-made MXene as multilayered 2D material, consistent with previous studies [21,28].

The zeta potential value of P-MXene from pH 3 to 11, which can represent the surface charge density of materials, is shown in Fig. S2. The surface of P-MXene becomes more negatively charged with increasing pH because the terminals of P-MXene (T_X) consists of -OH, -O, and/or -F [29]. The selected pharmaceuticals, which consist of single or multiple charged groups, have different species depending on each pKa value. Among them, the AMT and VRP (pKa: 9.76 and 9.68, respectively) have the strongest basic pKa with the amine group acting as an electron donor leading to protonation below their pKa [10]. On the other hand, the CBM, EE2, IBP, and DCF (pKa: 15.96, 10.33, 4.85, and 4.00, respectively), which have the strongest acidic pKa, can lose their proton below their pKa [11]. Adsorption is a mixed process influenced by properties of adsorbent and adsorbate [10]. Therefore, these indicate that solution pH is an important factor for adsorption performance because both P-MXene and pharmaceutical species can be changed, depending on the pH conditions.

Fig. 1 shows the adsorption performance on selected pharmaceuticals by P-MXene on pH 3.5, 7, and 10.5. The relative concentration (C/C₀) values in AMT and VRP were shown to be considerably lower than in CBM, EE2, IBP, and DCF in all pH conditions. The AMT and VRP indicated the best performance at pH 7 (C/C₀: 0.58 and 0.62, respectively) than pH 3.5 (C/ C_0 : 0.67 and 0.75, respectively) and pH 10.5 (C/ C_0 : 0.73 and 0.73, respectively). This could be due to the fact that at pH 3.5, although positively charged AMT and VRP was dominant, relatively lower negatively charged P-MXene was observed. In addition, at pH 10.5, a lower zeta potential value of P-MXene was shown, but most AMT and VRP existed in neutralized form. On the contrary, due to the dominance of positively charged AMT and VRP, and relatively higher negative charged P-MXene, AMT and VRP were more adsorbed on P-MXene at pH 7 due to electrostatic attraction. Furthermore, P-MXene exhibited better adsorption performance for AMT than VRP in all of the experiment's pH conditions. Numerous studies reported that the intercalation process on 2D materials like P-MXene is mostly affected by the size of target compounds [21,30,31]. This is presumably because VRP can rarely be relatively intercalated between layers of P-MXene due to its higher molecular volume than AMT (283 Å³ for AMT and 459 Å³ for

Meanwhile, the influence of pH conditions can be negligible on CBM, which is non-ionizable under all experiment pH conditions. However, EE2 was observed to slightly increase C/C_0 value from 0.88 at pH 3.5 and 7 to 0.90 at pH 10.5. In addition, IBP and DCF were shown to increase C/C_0 values from 0.88 and 0.89 at pH 3 to 0.92 and 0.93 at pH 7 and pH 10.5, respectively. These confirm that at a pH value above their pKa, the adsorption affinity decreases due to electrostatic repulsion between ionized pharmaceutical compounds and negatively charged P-MXene. Moreover, hydrophobic partitioning has been reported as one of the most effective mechanisms in organic compound adsorption [31]. However, because P-MXene possesses higher

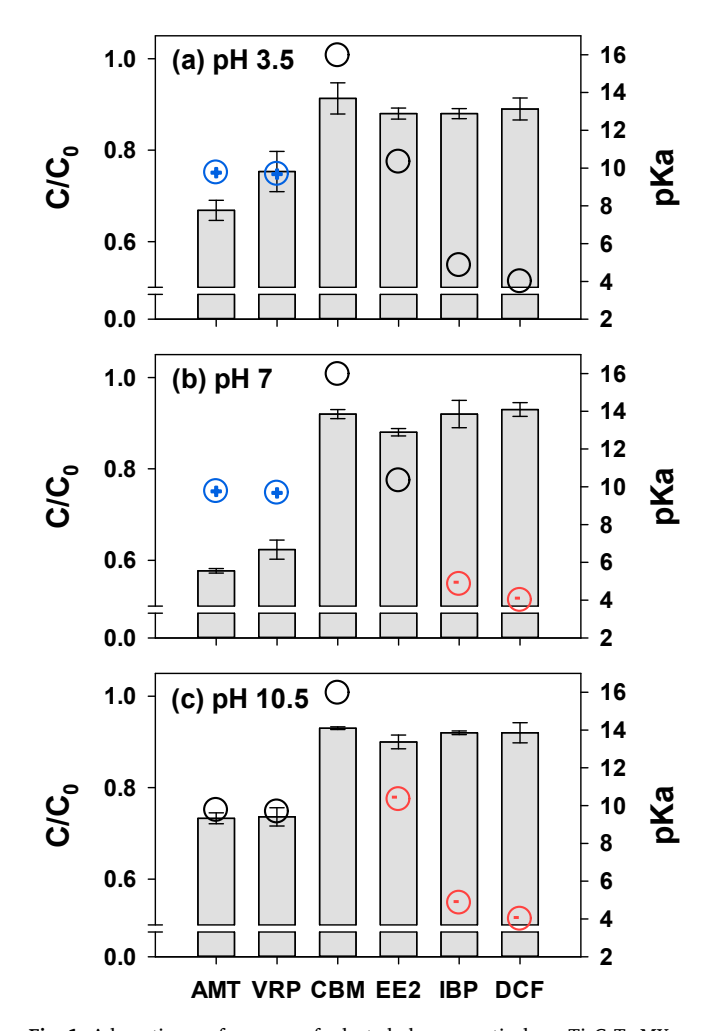


Fig. 1. Adsorption performance of selected pharmaceuticals on ${\rm Ti}_3C_2T_X$ MXene with pKa value; bars represent standard deviation of adsorption performance; circles represent pKa values of each pharmaceutical compound; positive charged compound (+), neutral compound (O), and negative charged compound (–) at each conducted pH condition.

hydrophilicity without aromatic rings, hydrophobic partitioning cannot be considered in this study. In addition, although hydrogen bonding between pharmaceutical compounds and the termination of P-MXene may have somewhat affected its adsorption performance [32], results showed the adsorbing of small amounts of neural or negatively charged pharmaceutical compounds. Therefore, in this study, the selected pharmaceutical adsorption performance that can primarily be explained by electrostatic interaction positively correlates with their charges by showing the highest removal for AMT at pH 7. In addition, plausible adsorption mechanisms of selected pharmaceutical compounds are shown in Fig. S3.

3.2. Influence of sonication frequency on adsorption performance

Based on its adsorption performance on different pharmaceutical compounds, P-MXene shows a potential to treat water with pharmaceutical compounds with higher performance observed for AMT at pH 7. To enhance adsorption performance, sonicated MXene at 28 and 580 kHz was applied for AMT at pH 7. Fig. 2 exhibits the adsorption kinetics and isotherm by P-MXene (0 kHz), S_{28} -MXene, and S_{580} -MXene, and each parameter is summarized in Tables S2 and S3. A higher adsorption performance was observed in sonicated MXene for both adsorption capacity and removal rate. This is because sonication makes well-dispersed MXene by producing cavitation bubbles, which

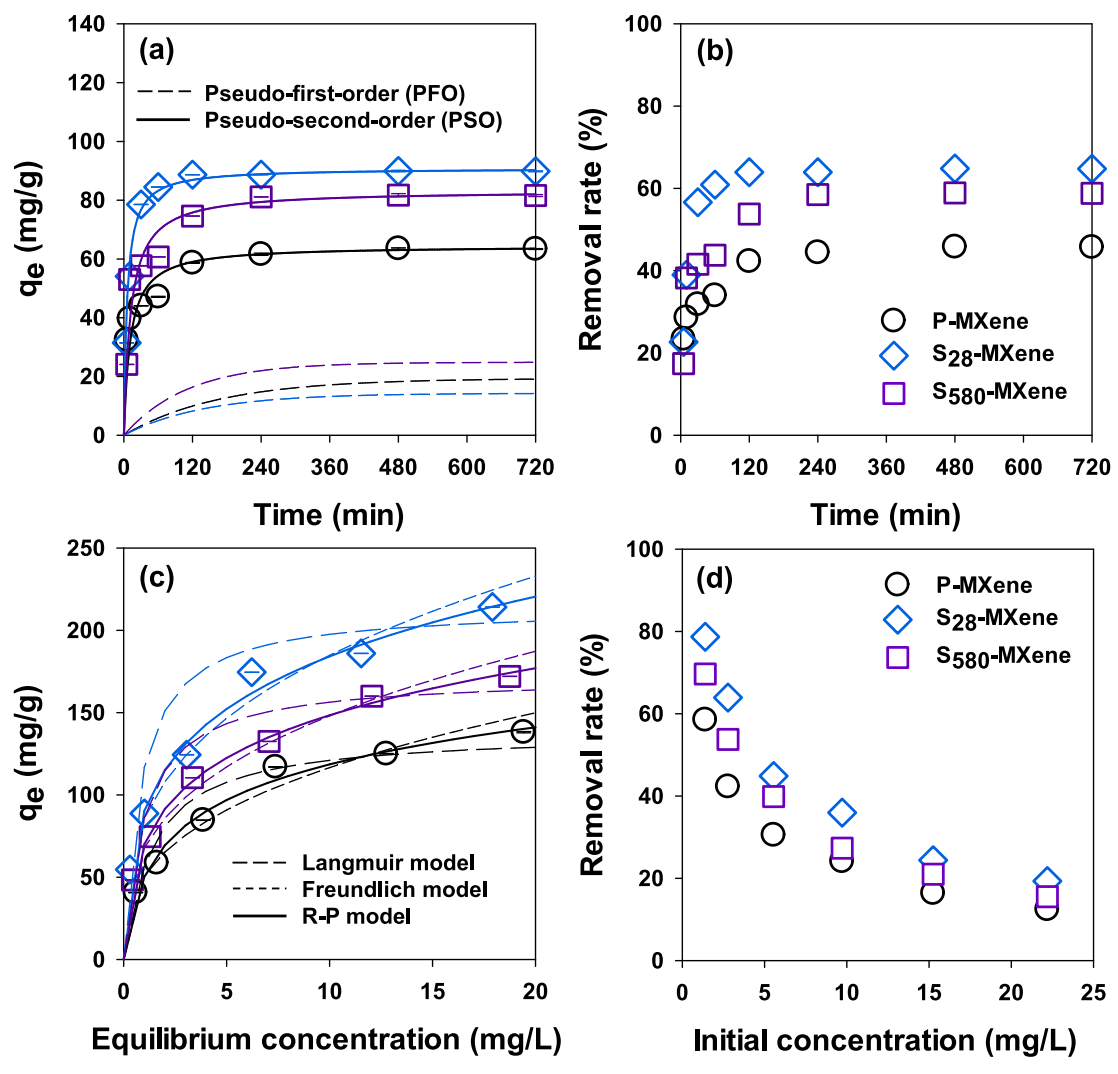
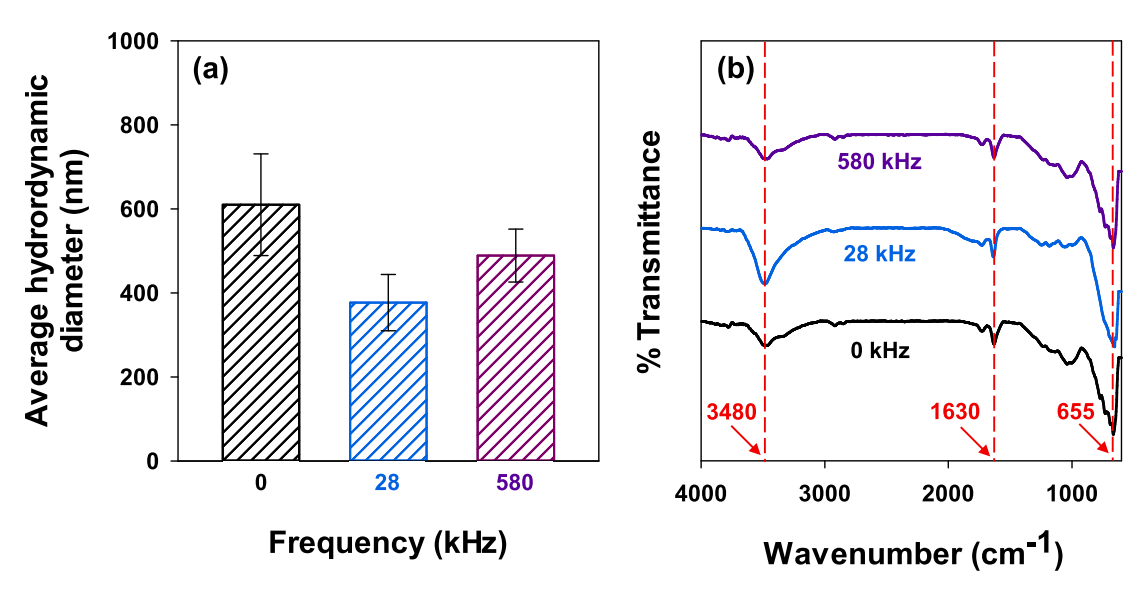


Fig. 2. Sonicated $Ti_3C_2T_X$ MXene adsorption performance for kinetics; (a) q_e vs. time and (b) removal rate vs. time; (c) q_e vs. c_e and with different models (d) removal rate vs. initial pharmaceuticals concentration. Error bars are smaller than the symbols in most cases.



 $\textbf{Fig. 3.} \ \, \textbf{(a)} \ \, \textbf{Hydrodynamic diameters by DLS and (b) FTIR spectrum variation of sonicated} \ \, \textbf{Ti}_{3}\textbf{C}_{2}\textbf{T}_{X} \ \, \textbf{MXene.}$

generates shock waves and shear forces by collapsing in the bulk solution [33,34]. In addition, by forming oxygenated functional groups like -OH and -COOH on the surface of sonicated MXene, it can positively affect adsorption performance. In particular, S28-MXene having the highest negatively surface by these functional group (estimated based on zeta potential value: see Fig. S2) showed the best performance. This result rises because the lower sonication frequency can produce relatively larger cavitation bubbles, which generates larger shock waves and shear forces [22,23]. Fig. 3a, which shows the hydrodynamic diameter of pristine and sonicated MXene, supports the finding that S28-MXene was more effective, by showing less aggregation. In addition, FTIR peaks (Fig. 3b) indicated that while similar Ti-O (655 cm⁻¹) functionality was shown with three different frequency conditions, more -OH (3480 cm⁻¹) and -COOH (1630 cm⁻¹) functional groups were shown in S28-MXene. This may increase the hydrogen bonding between MXene and AMT, resulting in improved removal. The TEM images, and XPS patterns, and zeta potential value of sonicated MXene further support this result, as shown in Fig. S2. The TEM images for highly-dispersed MXene and XPS patterns for higher oxygen contents, were observed in the following order: S₂₈-MXene > S₅₈₀-MXene > P-MXene. In particular, zeta potential value, which enables us to evaluate the MXene surface charge density, provides that by having the lowest value on S28-MXene, S28-MXene had the highest negative surface charge, resulting in higher electrostatic attraction with AMT. Furthermore, these results were consistent with reported studies that used single-walled carbon nanotubes [22] and graphene oxide [23] with sonication. Therefore, due to less aggregation and a higher amount of oxygenated functional groups on sonicated MXene, sonication can maximize the adsorption capacity of MXene.

In adsorption kinetics, the time taken to reach equilibrium status was observed to be approximately 120 min. In addition, the experimental adsorption capacities (qe, mg/g) were 64.0 for P-MXene, 90.1 for S28-MXene, and 81.6 for S580-MXene, which are similar to the calculated adsorption capacities by PSO (64.5, 90.9, and 83.3, respectively). Furthermore, the higher correlation coefficients (R^2) of PSO against that of PFO were presented for all three frequencies, which may indicate that the AMT adsorption mechanism of MXene is driven by chemisorption [35]. This result is consistent with the previously reported studies [31,33]. The adsorption isotherm was carried out to evaluate the AMT adsorption capacities by three kinds of MXene with initial concentration ranges of 1.39-22.2 mg/L. In addition, 120 min (pseudo-equilibrium time based on kinetic study) was applied. The maximum adsorption capacities (q_m, mg/g) of P-MXene, S₂₈-MXene, and S₅₈₀-MXene were found to be 138, 214, and 172, respectively. The lowest correlation coefficients (R2) value is shown on the Langmuir model, while the R-P model shows the highest R^2 value. In the R-P model, when β value is close to 1, the model resembles the Langmuir model, while, when $1/K_{\rm RP}$ value tends to 0, it resembles the Freundlich model. Due to the versatility of the R-P model, it can be used for either homogeneous or heterogeneous adsorption [36]. β values calculated in this study were 0.810, 0.763, and 0.780 for P-MXene, S28-MXene, and S₅₈₀-MXene, respectively, presenting weak fit the Langmuir model. However, by having 123, 487, and 267 of K_{RP} value, respectively, these adsorption isotherm results are more matching with the Freundlich model than with the Langmuir model. In addition, this indicates multilayer adsorption over heterogeneous MXene and these results are consistent with previous studies [31,32]. Lastly, these results were compared to other adsorption studies based on adsorption capacity, as shown in Table 1. The S28-MXene exhibits excellent AMT adsorption capacity, even better than carbon-based adsorbent, which is most commonly used.

3.3. Effect of various background inorganics and organics

Because contaminants exist with various ions in the surface water environment, the effect of various ions on adsorption performance was

 Table 1

 Comparison of the adsorption performance with the various adsorbent for AMT.

Adsorbent	C ₀ (mg/L)	q_m (mg/g)	pН	Reference
Palygorskite	1.59	52.7	6–7	[60]
Metal organic frameworks	277	27.7	6.0	[61]
Activated charcoal	0-200	181	6.5	[55]
Fe ₃ O ₄ @SiO ₂ -molecular imprinted polymer	6.94	12.2	8.0	[62]
Microalgae chlorella vulgari	0.690-27.7	16.6	6.5	[63]
PAC	5-20	231	7.0	[64]
Granular activated carbon		178		
Sonicated Ti ₃ C ₂ T _X MXene	0-22.2	241	7.0	This study

evaluated for AMT at pH 7 by S28-MXene. Fig. 4a shows the adsorption capacity variation with various inorganic ions. NaCl, NaHCO₃, NaNO₃, Na₂SO₄, and CaCl₂ as background inorganics were selected due to their availability in real aquatic systems [37]. The adsorption capacity with all five electrolytes was lower than without electrolytes. This result can be explained by the interaction between the adsorbent and adsorbate, which was screened with ionic strength increase (screening effect) [33]. In other words, the electrical double layer was compressed by higher ionic strength, leading to a weakened electrostatic interaction between S₂₈-MXene and AMT. Among five inorganics, monovalent ions (NaCl, NaHCO3, and NaNO3) showed the smallest effect on the adsorption capacity (81.7, 82.1, and 81.3 mg/g, respectively) compared to the absence of background ions. This is due to the fact that although there was a competition between Na+ and AMT+ to be adsorbed on the S28-MXene, Na+ as a monovalent ion can be relatively less effective than divalent cation [38]. In addition, Na₂SO₄ as a divalent anionic ion had a slightly more negative influence on the adsorption capacity (80.8 mg/g) than monovalent ions. When Na₂SO₄ ions were present in the solution, SO₄² was shown to complex with some parts of AMT⁺ to form SO₄AMT in terms of electrostatic status, resulting in less electrostatic affinity to S₂₈-MXene [39,40]. The adsorption capacity with CaCl₂ was the lowest among those salts (1, 2, 3, 4, and 6 meq/L for 77.1, 73.6, 70.7, 68.8, and 67.0 mg/g, respectively). This is due to a relatively strong competition between Ca2+ as a divalent cation and AMT+ for adsorption sites on S28-MXene [38]. In addition, another plausible reason could be due to a salting-out effect, in which the hydrophobic interaction between organic compounds can induce a higher ionic strength in the solution [41]. Due to the salting-out effect, reduced solubility of AMT can cause a larger molecular size and/or precipitation of some AMT, resulting in hardly any adsorption. Furthermore, this effect can be empirically calculated by Setschenow constants [42,43], which is described in Section 4 in detail. The solubility of AMT with CaCl2 decreased from 6,547 to 6,483 mg/L, with increasing CaCl2 concentration from 1 to 6 meq/L, respectively, as shown in Fig. S4a. This calculated solubility supports the theory that increased CaCl₂ concentration in the solution can negatively impact on adsorption capacity. Additionally, it was observed that adsorption capacity decreased following an exponential decay, with increased CaCl₂ concentration. This observation can be explained by the Debye length decreasing as the ion concentration increases. The Debye length, which represents the range of electrical double layer thickness, directly relates to electrostatic interaction between adsorbent and adsorbate [42,44]. Fig. S4b shows that the calculated Debye length exponentially decreased as the concentration of CaCl2 was further increased. Consequently, while inorganics in solutions can influence adsorption capacity, an increase in ion concentration can lead to less effective adsorption performance.

To assess the effect of background organics in adsorption processes, the adsorption capacity with HA, TA, and CPC is shown in Fig. 4b. The humic acid (HA) and tannic acid (TA), which are ubiquitous organic compounds as NOM [23], and CPC, which are major cationic surfactant constituents of the pharmaceutical industry and easily discharged into

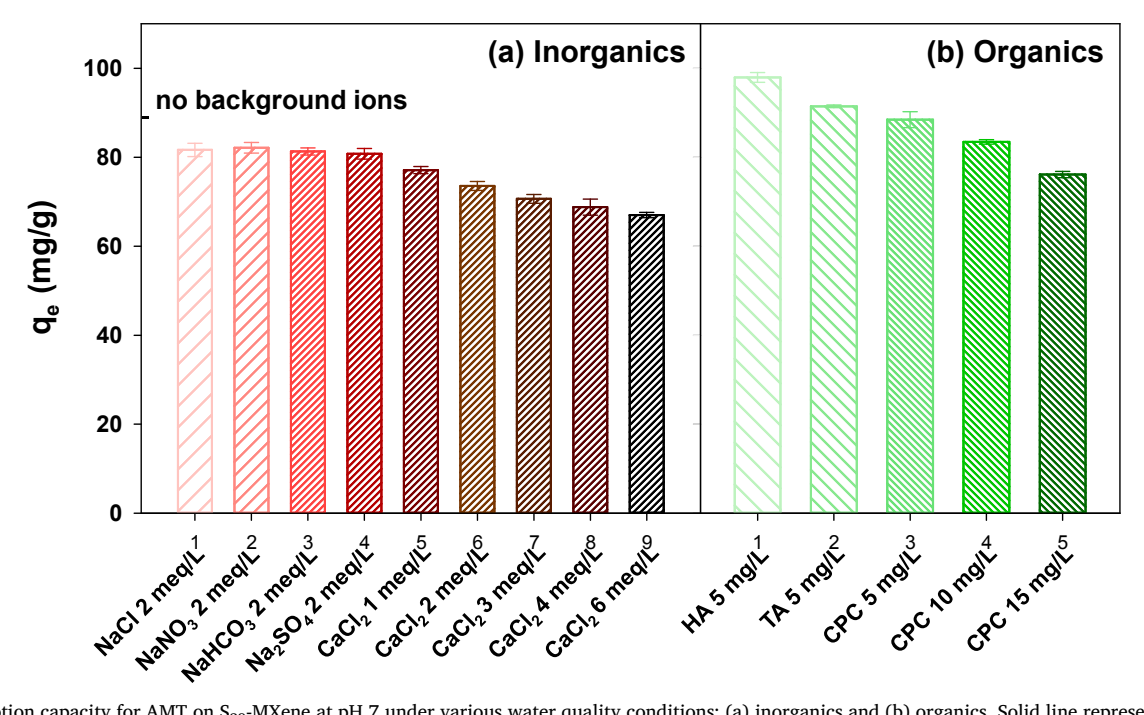


Fig. 4. Adsorption capacity for AMT on S_{28} -MXene at pH 7 under various water quality conditions; (a) inorganics and (b) organics. Solid line represents adsorption capacity of no background ions or organics for AMT on S_{28} -MXene at pH 7.

natural water [45], were selected as background organics. The results of adsorption capacity with HA or TA (97.9 and 91.5 mg/g, respectively) were shown to be slightly higher than without background compounds. This observation is in accordance with a plethora of research that HA or TA could interact with organic contaminants, leading to increased adsorption capacity [46-48]. This is possible due to a hydrophobic interaction between AMT and HA or TA, which have aromatic rings and non-polar aliphatic carbon chains [49]. In addition, the dissociation protons of carboxylic and phenolic functional groups of HA or TA results in negative charges, which can generate electrostatic repulsion between HA or TA and termination of S28-MXene, and can play a role in inducing AMT-HA or TA binding [46,49]. Furthermore, adsorption capacity with HA was higher than that with TA due to a relatively higher hydrophobicity, stronger negative charge, and bigger HA [50,51]. On the other hand, while adsorption capacity of the lowest CPC concentration (88.5 mg/g) was similar with that of no ions, the overall adsorption capacity was gradually decreased by increasing CPC concentration in the solution (10 and 15 mg/L for 83.5 and 76.1 mg/g, respectively). This may be explained by the competition between AMT and cationic CPC monomers on adsorption sites of S28-MXene being the more dominant mechanism. In addition, this suggests that hydrophobic interactions between AMT and adsorbed CPC on S28-MXene by ionpairing are likely not major mechanisms in this adsorption process [26,52]. Therefore, these results indicate that electrostatic interaction should be considered in the application of S28-MXene for pharmaceutical compounds' adsorption.

3.4. Comparison of performance between sonicated ${\rm Ti}_3 C_2 {\rm T}_X$ MXene and PAC

Adsorption capacity comparison between sonication-assisted S_{28} -MXene and commercial PAC was conducted to confirm that S_{28} -MXene is an effective alternative to PAC at pH 7, as shown in Fig. 5. AMT, EE2, and IBP were selected due to their differing hydrophobicity and ionic forms. Hydrophobic and hydrophilic interaction (*i.e.*, hydrogen bonding and electrostatic interaction) were known as the main adsorption mechanism on PAC for organic compounds [53]. The adsorption capacity for IBP on PAC (60.3 mg/g) was slightly lower than that for AMT

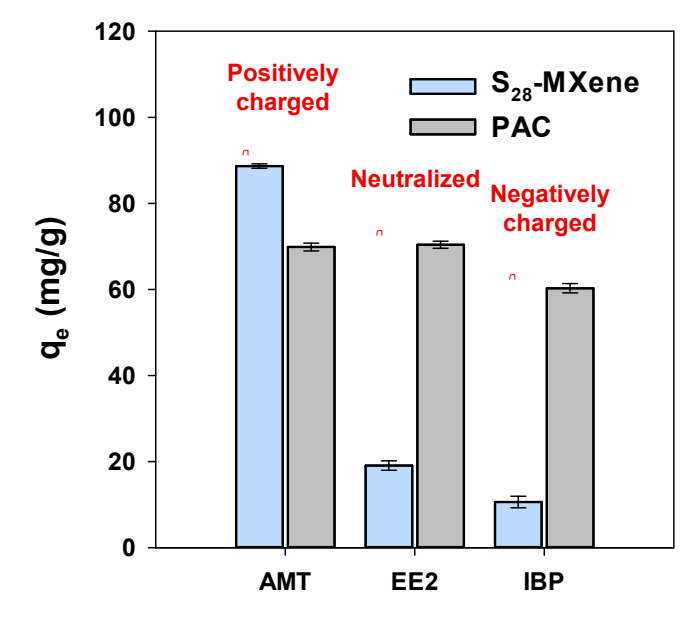


Fig. 5. Comparison of S_{28} -MXene and PAC adsorption capacity for AMT, EE2, and IBP at pH 7.

(69.9 mg/g) and EE2 (70.4 mg/g) due not only to less hydrophobicity, which is represented by octanol–water partitioning coefficient (log $K_{\rm OW}$); 4.81 for AMT, 3.90 for EE2, and 3.84 for IBP but also to electrostatic repulsion between IBP and PAC. In addition, adsorption performance for AMT and EE2 was observed to be similar in PAC. Because log $K_{\rm OW}$ is only estimated for the neutral molecular form, hydrophobicity of ionized AMT may be lower than that of neutralized AMT [54]. Furthermore, it was reported that log $K_{\rm OW}$ of some cationic pharmaceuticals could not positively correlate with adsorption performance on PAC [55]. For hydrophilic interaction, while it exhibits less hydrogen bonding acceptor and donor on AMT than EE2, it can additionally induce electrostatic attraction AMT as amphiphilic compounds and PAC. Therefore, presumably, due to the tradeoff between these mechanisms, AMT and EE2 had similar adsorption capacities,

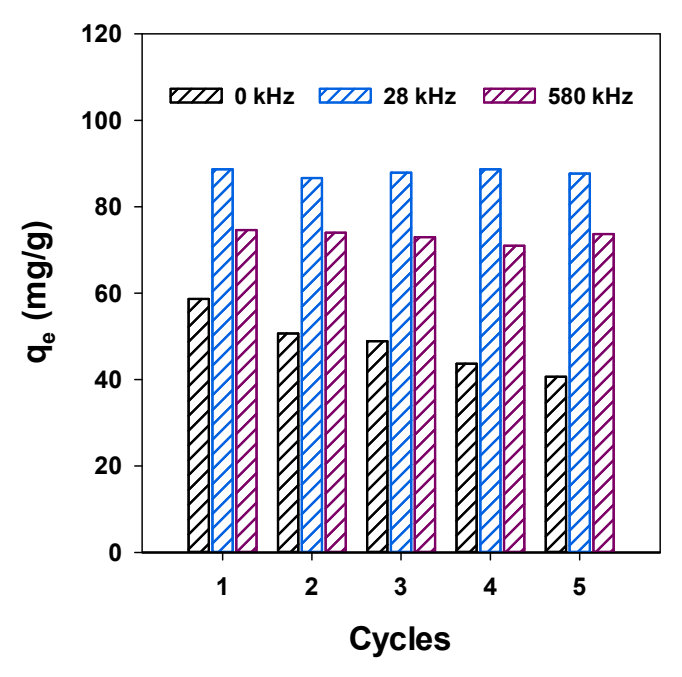


Fig. 6. Reusability of pristine and sonicated ${\rm Ti_3C_2T_X}$ MXene for AMT adsorption at pH 7.

slightly higher than IBP.

AMT can be more adsorbed on S_{28} -MXene by electrostatic attraction than EE2 and IBP, similar to P-MXene, as earlier mentioned. In addition, the adsorption performance of AMT on S_{28} -MXene was indicated as higher than PAC's. This is probably because AMT is more likely to be adsorbed on the more negatively charged surface of S_{28} -MXene than PAC. In addition, the limitations of PAC, such as slow kinetics and poor performance for polar organic compounds can arise this result [13]. However, due to electrostatic interaction, adsorption capacity for EE2 and IBP on S_{28} -MXene was measured lower than on PAC. As a result, the strong selectivity of MXene is confirmed through these results and is useful in practical terms for various water treatments.

3.5. Recyclability of Ti₃C₂T_X MXene

From an economic perspective, the recyclability of adsorbents should be considered in water treatment plants. The adsorption capacity for AMT on recycled MXene by rinsing with HCl, NaOH, and DI water was evaluated, as presented in Fig. 6. The adsorption capacity on P-MXene gradually decreased with increased cycles from 58.7 mg/g to 40.6 mg/g. However, sonicated MXene remained relatively stable during 5 cycles. Although exact cost comparison is somewhat difficult due to sever cost dropping of Ti₃C₂T_X MXene as very new material, sonicated MXene could be superior based on economic perspective. The improved performance on the recyclability of MXene by sonication can be due to weakened binding energy between adsorbed AMT and sonicated MXene. The cavitation bubbles caused by ultrasonic irradiation can generate a whirlpool action [56,57] and increase the solution temperature [58,59], leading to higher desorption. Furthermore, powder adsorbents, which are generally applied early in conventional drinking water treatment, can be subsequently removed by both sedimentation and filtration. Therefore, sonicated MXene could be confirmed as not only having superior adsorption capacity and high selectivity but also safety and better disposal or reusability.

4. Conclusions

In this study, multilayered 2D ${\rm Ti_3C_2T_X}$ MXene was applied to treat pharmaceutical compounds in adsorption systems. Among selected

pharmaceutical compounds, AMT and VRP showed higher adsorption performance. In addition, at pH 7, these compounds had relatively higher positive charges, and pristine MXene (P-MXene) had a relatively higher negatively-charged surface, resulting in the highest performance. These results indicated that electrostatic attraction was observed as the dominant adsorption mechanism through the strong negatively-charged surface on P-MXene. In addition, to improve adsorption performance, sonicated MXene at 28 and 580 kHz (S28-MXene and S₅₈₀-MXene) was compared with P-MXene for AMT at pH 7. By showing a smaller well-dispersed, hydrodynamic diameter and higher oxygenated functional groups on sonicated MXene, the maximum adsorption capacity was observed to be highest at 28 kHz compared to that at 580 kHz and no sonication. Because larger cavitation bubbles were generated at lower frequencies, S28-MXene exhibited higher performance. The adsorption performance experiments, without ions and with background ions, were conducted for AMT by S28-MXene. The adsorption capacity with background inorganics was lower than that without ions because these ions screened electrostatic interaction between AMT and MXene. While adsorption capacity with NOM was higher, the capacity with CPC was lower than one without ions due to the competition between CPC and AMT. Although there was almost no adsorption capacity difference caused by PAC, the adsorption capacity for AMT was higher than that for EE2 and IBP by S_{28} -MXene. This result supported evidence of the high selectivity of MXene. In addition, the sonicated MXene indicated insignificant reduced adsorption capacity with the number of recycles. These results can be useful for long term MXene study. Therefore, sonicated MXene can be suggested as an alternative and effective adsorbent of pharmaceutical compounds as it has shown high performance, selectivity, and reusability.

Declaration of Competing Interest

The authors declare that they have no known competing financial interests or personal relationships that could have appeared to influence the work reported in this paper.

Acknowledgments

This research was also supported by the Korea Ministry of Environment, 'The SEM projects; 2018002470005, South Korea'. This research was also supported by the National Science Foundation, USA (OIA-1632824).

Appendix A. Supplementary data

Supplementary data to this article can be found online at https://doi.org/10.1016/j.cej.2020.126789.

References

- [1] S. Kim, K.H. Chu, Y.A. Al-Hamadani, C.M. Park, M. Jang, D.-H. Kim, M. Yu, J. Heo, Y. Yoon, Removal of contaminants of emerging concern by membranes in water and wastewater: a review, Chem. Eng. J. 335 (2018) 896–914.
- [2] E.T. Hester, A.-Y.-C. Lin, C.W. Tsai, Effect of floodplain restoration on photolytic removal of pharmaceuticals, Environ. Sci. Technol. 54 (6) (2020) 3278–3287.
- [3] D.W. Kolpin, E.T. Furlong, M.T. Meyer, E.M. Thurman, S.D. Zaugg, L.B. Barber, H.T. Buxton, Pharmaceuticals, hormones, and other organic wastewater contaminants in US streams, 1999–2000: a national reconnaissance, Environ. Sci. Technol. 36 (2002) 1202–1211.
- [4] Y. Li, J.B. Sallach, W. Zhang, S.A. Boyd, H. Li, Insight into the distribution of pharmaceuticals in soil-water-plant systems, Water Res. 152 (2019) 38–46.
- [5] X. Bai, A. Lutz, R. Carroll, K. Keteles, K. Dahlin, M. Murphy, D. Nguyen, Occurrence, distribution, and seasonality of emerging contaminants in urban watersheds, Chemosphere 200 (2018) 133–142.
- [6] L.M. Bexfield, P.L. Toccalino, K. Belitz, W.T. Foreman, E.T. Furlong, Hormones and pharmaceuticals in groundwater used as a source of drinking water across the United States, Environ. Sci. Technol. 53 (2019) 2950–2960.
- [7] Y. Yang, Y.S. Ok, K.-H. Kim, E.E. Kwon, Y.F. Tsang, Occurrences and removal of pharmaceuticals and personal care products (PPCPs) in drinking water and water/ sewage treatment plants: a review, Sci. Total Environ. 596 (2017) 303–320.
- [8] G. Cerreta, M.A. Roccamante, P. Plaza-Bolaños, I. Oller, A. Aguera, S. Malato,

- L. Rizzo, Advanced treatment of urban wastewater by UV-C/free chlorine process: Micro-pollutants removal and effect of UV-C radiation on trihalomethanes formation, Water Res. 169 (2020) 115220.
- [9] K. Manoli, L.M. Morrison, M.W. Sumarah, G. Nakhla, A.K. Ray, V.K. Sharma, Pharmaceuticals and pesticides in secondary effluent wastewater: Identification and enhanced removal by acid-activated ferrate (VI), Water Res. 148 (2019) 272-280.
- [10] R. Guillossou, J. Le Roux, R. Mailler, C.S. Pereira-Derome, G. Varrault, A. Bressy, E. Vulliet, C. Morlay, F. Nauleau, V. Rocher, Influence of dissolved organic matter on the removal of 12 organic micropollutants from wastewater effluent by powdered activated carbon adsorption, Water Res. 115487 (2020).
- [11] C. Jung, J. Park, K.H. Lim, S. Park, J. Heo, N. Her, J. Oh, S. Yun, Y. Yoon, Adsorption of selected endocrine disrupting compounds and pharmaceuticals on activated biochars, J. Hazard. Mater. 263 (2013) 702–710.
- [12] J. Zhou, F. Ma, H. Guo, Adsorption behavior of tetracycline from aqueous solution on ferroferric oxide nanoparticles assisted powdered activated carbon, Chem. Eng. J. 384 (2020) 123290.
- [13] Y. Ling, D.M. Alzate-Sánchez, M.J. Klemes, W.R. Dichtel, D.E. Helbling, Evaluating the effects of water matrix constituents on micropollutant removal by activated carbon and β -cyclodextrin polymer adsorbents, Water Res. 173 (2020) 115551.
- [14] F. Bonvin, L. Jost, L. Randin, E. Bonvin, T. Kohn, Super-fine powdered activated carbon (SPAC) for efficient removal of micropollutants from wastewater treatment lant effluent, Water Res. 90 (2016) 90-99.
- A.M. Kennedy, R.S. Summers, Effect of DOM size on organic micropollutant adsorption by GAC, Environ. Sci. Technol. 49 (2015) 6617–6624. L. Zhao, B. Dong, S. Li, L. Zhou, L. Lai, Z. Wang, S. Zhao, M. Han, K. Gao, M. Lu,
- Interdiffusion reaction-assisted hybridization of two-dimensional metal-organic frameworks and Ti₃C₂T_x nanosheets for electrocatalytic oxygen evolution, ACS Nano 11 (2017) 5800-5807.
- [17] B.-M. Jun, S. Kim, J. Heo, C.M. Park, N. Her, M. Jang, Y. Huang, J. Han, Y. Yoon, Review of MXenes as new nanomaterials for energy storage/delivery and selected environmental applications, Nano Res. 12 (2019) 471-487.
- [18] H. Jiang, Z. Wang, Q. Yang, M. Hanif, Z. Wang, L. Dong, M. Dong, A novel MnO₂/ Ti₂C₂T₂ MXene nanocomposite as high performance electrode materials for flexible supercapacitors, Electrochim. Acta 290 (2018) 695–703.
- [19] I. Ihsanullah, MXenes (two-dimensional metal carbides) as emerging nanomaterials for water purification: Progress, challenges and prospects, Chem. Eng. J. 388 (15) 2020) 124340
- [20] K. Rasool, R.P. Pandey, P.A. Rasheed, G.R. Berdiyorov, K.A. Mahmoud, MXenes for Environmental and Water Treatment Applications, in: 2D Metal Carbides and Nitrides (MXenes), Springer 2019, pp. 417-444.
- [21] M.R. Lukatskava, O. Mashtalir, C.F. Ren, Y. Dall'Agnese, P. Rozier, P.L. Taberna, M. Naguib, P. Simon, M.W. Barsoum, Y. Gogotsi, Cation intercalation and high volumetric capacitance of two-dimensional titanium carbide, Science 341 (2013) 1502-1505.
- C.M. Park, Y.A. Al-Hamadani, J. Heo, N. Her, K.H. Chu, M. Jang, S. Lee, Y. Yoon, Aggregation kinetics of single walled carbon nanotubes influenced by the frequency of ultrasound irradiation in the aquatic environment, Ultrason. Sonochem. 39 (2017) 750-757.
- [23] S.-W. Nam, C. Jung, H. Li, M. Yu, J.R. Flora, L.K. Boateng, N. Her, K.-D. Zoh, Y. Yoon, Adsorption characteristics of diclofenac and sulfamethoxazole to graphene oxide in aqueous solution, Chemosphere 136 (2015) 20-26.
- [24] J. Hilding, E.A. Grulke, Z. George Zhang, F. Lockwood, Dispersion of carbon nanotubes in liquids, J. Dispers. Sci. Technol. 24 (2003) 1-41.
- [25] H. Peltenburg, N. Timmer, I.J. Bosman, J.L. Hermens, S.T. Droge, Sorption of structurally different ionized pharmaceutical and illicit drugs to a mixed-mode coated microsampler, J. Chromatogr. A 1447 (2016) 1-8.
- S. Kim, C.M. Park, A. Jang, M. Jang, A.J. Hernández-Maldonado, M. Yu, J. Heo, Y. Yoon, Removal of selected pharmaceuticals in an ultrafiltration-activated biochar hybrid system, J. Membr. Sci. 570 (2019) 77-84.
- [27] A. Shahzad, K. Rasool, W. Miran, M. Nawaz, J. Jang, K.A. Mahmoud, D.S. Lee, Mercuric ion capturing by recoverable titanium carbide magnetic nanocomposite, J. Hazard, Mater. 344 (2018) 811-818.
- [28] M. Hu, T. Hu, Z. Li, Y. Yang, R. Cheng, J. Yang, C. Cui, X. Wang, Surface functional groups and interlayer water determine the electrochemical capacitance of Ti₃C₂T_x MXene, ACS Nano 12 (2018) 3578-3586.
- [29] Z. Ling, C.E. Ren, M.-Q. Zhao, J. Yang, J.M. Giammarco, J. Qiu, M.W. Barsoum, Y. Gogotsi, Flexible and conductive MXene films and nanocomposites with high apacitance, PNAS 111 (2014) 16676-16681.
- [30] J. Wan, S.D. Lacey, J. Dai, W. Bao, M.S. Fuhrer, L. Hu, Tuning two-dimensional nanomaterials by intercalation: materials, properties and applications, Chem. Soc. Rev. 45 (2016) 6742-6765.
- [31] O. Mashtalir, K.M. Cook, V.N. Mochalin, M. Crowe, M.W. Barsoum, Y. Gogotsi, Dye adsorption and decomposition on two-dimensional titanium carbide in aqueous nedia, J. Mater. Chem. A 2 (2014) 14334-14338.
- [32] F. Meng, M. Seredych, C. Chen, V. Gura, S. Mikhalovsky, S. Sandeman, G. Ingavle, T. Ozulumba, L. Miao, B. Anasori, MXene sorbents for removal of urea from dialysate: a step toward the wearable artificial kidney, ACS Nano 12 (2018) 10518-10528.
- [33] K.H. Chu, Y.A. Al-Hamadani, C.M. Park, G. Lee, M. Jang, A. Jang, N. Her, A. Son, . Yoon, Ultrasonic treatment of endocrine disrupting compounds, pharmace ticals, and personal care products in water: a review, Chem. Eng. J. 327 (2017)
- [34] M. Burns, L.N. Marin, P.A. Schneider, Investigations of a continuous Poiseuille flow struvite seed crystallizer-Mixer performance and aggregate disruption by sonication, Chem. Eng. J. 295 (2016) 552–562.

 A. Belalia, A. Zehhaf, A. Benyoucef, Preparation of hybrid material based of PANI
- with SiO 2 and its adsorption of phenol from aqueous solution, Polym. Sci. Ser. B 60

- (2018) 816-824.
- [36] K.Y. Foo, B.H. Hameed, Insights into the modeling of adsorption isotherm systems, Chem. Eng. J. 156 (2010) 2-10.
- [37] S. Kim, C.M. Park, M. Jang, A. Son, N. Her, M. Yu, S. Snyder, D.-H. Kim, Y. Yoon, Aqueous removal of inorganic and organic contaminants by graphene-based nanoadsorbents: a review, Chemosphere 212 (2018) 1104–1124.
- [38] L.D. Nghiem, A.I. Schäfer, M. Elimelech, Role of electrostatic interactions in the retention of pharmaceutically active contaminants by a loose nanofiltration membrane, J. Membr. Sci. 286 (2006) 52-59.
- [39] K.-L. Chen, L.-C. Liu, W.-R. Chen, Adsorption of sulfamethoxazole and sulfapyridine antibiotics in high organic content soils, Environ. Pollut. 231 (2017) 1163-1171.
- J. Akhtar, N.A.S. Amin, K. Shahzad, A review on removal of pharmaceuticals from water by adsorption, Desalin. Water Treat. 57 (2016) 12842-12860.
- [41] A. Burant, G.V. Lowry, A.K. Karamalidis, Measurement of Setschenow constants for six hydrophobic compounds in simulated brines and use in predictive modeling for oil and gas systems, Chemosphere 144 (2016) 2247-2256.
- [42] X. Wu, P. Liu, H. Huang, S. Gao, Adsorption of triclosan onto different aged polypropylene microplastics: Critical effect of cations, Sci. Total Environ. 717 (2020) 137033
- [43] J. Setschenow, Über die konstitution der salzlösungen auf grund ihres verhaltens zu kohlensäure, Zeitschrift für Physikalische Chemie 4 (1889) 117-125.
- R. Guégan, T. De Oliveira, J. Le Gleuher, Y. Sugahara, Tuning down the environmental interests of organoclays for emerging pollutants: Pharmaceuticals in presence of electrolytes, Chemosphere 239 (2020) 124730.

 A.C. Hari, R.A. Paruchuri, D.A. Sabatini, T.C. Kibbey, Effects of pH and cationic and
- nonionic surfactants on the adsorption of pharmaceuticals to a natural aquifer material, Environ. Sci. Technol. 39 (2005) 2592-2598.
- [46] J. Jin, T. Feng, R. Gao, Y. Ma, W. Wang, Q. Zhou, A. Li, Ultrahigh selective adsorption of zwitterionic PPCPs both in the absence and presence of humic acid: performance and mechanism, J. Hazard. Mater. 348 (2018) 117-124.
- [47] Z. Zhu, J. Xie, M. Zhang, Q. Zhou, F. Liu, Insight into the adsorption of PPCPs by porous adsorbents: Effect of the properties of adsorbents and adsorbates, Environ. Pollut, 214 (2016) 524-531.
- [48] L. Aristilde, G. Sposito, Complexes of the antimicrobial ciprofloxacin with soil, peat, and aquatic humic substances, Environ. Toxicol. Chem. 32 (2013) 1467–1478.
- [49] L.D. Nghiem, D. Vogel, S. Khan, Characterising humic acid fouling of nanofiltration membranes using bisphenol A as a molecular indicator, Water Res. 42 (2008) 4049-4058
- [50] C. Jung, N. Phal, J. Oh, K.H. Chu, M. Jang, Y. Yoon, Removal of humic and tannic acids by adsorption-coagulation combined systems with activated biochar, J. Hazard, Mater. 300 (2015) 808-814.
- [51] S. Kim, J.C. Muñoz-Senmache, B.-M. Jun, C.M. Park, A. Jang, M. Yu, A.J. Hernández-Maldonado, Y. Yoon, A metal organic framework-ultrafiltration hybrid system for removing selected pharmaceuticals and natural organic matter, Chem. Eng. J. 382 (2020) 122920.
- [52] T. De Oliveira, R. Guégan, T. Thiebault, C. Le Milbeau, F. Muller, V. Teixeira, M. Giovanela, M. Boussafir, Adsorption of diclofenac onto organoclays: Effects of surfactant and environmental (pH and temperature) conditions, J. Hazard. Mater. 323 (2017) 558-566.
- J. Löwenberg, A. Zenker, M. Baggenstos, G. Koch, C. Kazner, T. Wintgens, Comparison of two PAC/UF processes for the removal of micropollutants from wastewater treatment plant effluent: process performance and removal efficiency, Water Res. 56 (2014) 26-36.
- P. Westerhoff, Y. Yoon, S. Snyder, E. Wert, Fate of endocrine-disruptor, pharmaceutical, and personal care product chemicals during simulated drinking water treatment processes, Environ. Sci. Technol. 39 (2005) 6649–6663.
- Y. Zhao, J.-W. Choi, J.K. Bediako, M.-H. Song, S. Lin, C.-W. Cho, Y.-S. Yun, Adsorptive interaction of cationic pharmaceuticals on activated charcoal: Experimental determination and QSAR modelling, J. Hazard. Mater. 360 (2018) 529-535
- [56] D.-S. Kwon, S.-Y. Tak, J.-E. Lee, M.-K. Kim, Y.H. Lee, D.W. Han, S. Kang, K.-D. Zoh, Desorption of micropollutant from spent carbon filters used for water purifier, Environ. Sci. Pollut. Res. 24 (2017) 17606-17615.
- C. Zhou, N. Gao, R. Li, Y. Deng, Desorption of bisphenol-A (BPA) and regeneration of BPA-spent granular activated carbon using ultrasonic irradiation and organic solvent extraction, Desalin. Water Treat. 54 (2015) 3106-3113.
- [58] G. Cornelissen, P.C. van Noort, J.R. Parsons, H.A. Govers, Temperature dependence of slow adsorption and desorption kinetics of organic compounds in sediments Environ. Sci. Technol. 31 (1997) 454–460.
- [59] M. Breitbach, D. Bathen, H. Schmidt-Traub, Effect of ultrasound on adsorption and desorption processes, Ind. Eng. Chem. Res. 42 (2003) 5635-5646.
- Y.-L. Tsai, P.-H. Chang, Z.-Y. Gao, X.-Y. Xu, Y.-H. Chen, Z.-H. Wang, X.-Y. Chen, Z. . Yang, T.-H. Wang, J.-S. Jean, Amitriptyline removal using palygorskite clay, Chemosphere 155 (2016) 292-299.
- S. Lin, Y. Zhao, Y.-S. Yun, Highly Effective Removal of nonsteroidal anti-inflammatory pharmaceuticals from Water by Zr (IV)-Based Metal-Organic Framework: adsorption performance and mechanisms, ACS Appl. Mater. Inter. 10 (2018) 28076–28085.
- [62] K. Kamari, A. Taheri, Preparation and evaluation of magnetic core-shell mesoporous molecularly imprinted polymers for selective adsorption of amitriptyline in biological samples, J. Taiwan Inst. Chem. E 86 (2018) 230–239.
- [63] C.-W. Cho, Y. Zhao, Y.-S. Yun, QSAR modelling for predicting adsorption of neutral, cationic, and anionic pharmaceuticals and other neutral compounds to microalgae Chlorella vulgaris in aquatic environment, Water Res. 151 (2019) 288-295.
- F.J. Real, F.J. Benitez, J.L. Acero, F. Casas, Adsorption of selected emerging contaminants onto PAC and GAC: Equilibrium isotherms, kinetics, and effect of the water matrix, J. Environ. Sci. Health A 52 (2017) 727-734.